

# Mitotic accumulations of PML protein contribute to the re-establishment of PML nuclear bodies in G1

Graham Dellaire\*, Christopher H. Eskiw\*, Hesam Dehghani†, Reagan W. Ching and David P. Bazett-Jones§

Programme in Cell Biology, The Hospital for Sick Children, 555 University Avenue, Toronto, Ontario, M5G 1X8, Canada

\*These authors contributed equally to this work

†Present address: Department of Physiology, School of Veterinary Medicine, Ferdowsi University of Mashhad, Mashhad, Iran

§Author for correspondence (e-mail: dbjones@sickkids.ca)

Accepted 30 November 2005

Journal of Cell Science 119, 1034-1042 Published by The Company of Biologists 2006

doi:10.1242/jcs.02817

## Summary

Although the mechanism of chromosomal segregation is well known, it is unclear how other nuclear compartments such as promyelocytic leukemia (PML) nuclear bodies partition during mitosis and re-form in G1. We demonstrate that PML nuclear bodies partition via mitotic accumulations of PML protein (MAPPs), which are distinct from PML nuclear bodies in their dynamics, biochemistry and structure. During mitosis PML nuclear bodies lose biochemical components such as SUMO-1 and Sp100. We demonstrate that MAPPs are also devoid of Daxx and these biochemical changes occur prior to chromatin condensation and coincide with the loss of nuclear membrane integrity. MAPPs are highly mobile, yet do not readily exchange PML protein as demonstrated by fluorescence recovery after photo-bleaching (FRAP). A subset of MAPPs remains associated with mitotic chromosomes, providing a possible nucleation site for PML nuclear body formation in G1. As the nuclear envelope reforms in late anaphase, these nascent PML nuclear

bodies accumulate components sequentially, for example Sp100 and SUMO-1 before Daxx. After cytokinesis, MAPPs remain in the cytoplasm long after the reincorporation of splicing components and their disappearance coincides with new PML nuclear body formation even in the absence of new protein synthesis. The PML protein within MAPPs is not degraded during mitosis but is recycled to contribute to the formation of new PML nuclear bodies in daughter nuclei. The recycling of PML protein from one cell cycle to the next via mitotic accumulations may represent a common mechanism for the partitioning of other nuclear bodies during mitosis.

Supplementary material available online at

<http://jcs.biologists.org/cgi/content/full/119/6/1034/DC1>

Key words: Mitosis, PML nuclear bodies, Electron spectroscopic imaging, Proteasome inhibition

## Introduction

During metazoan cell division, the nucleus undergoes dramatic reorganisation and disassembly in an 'open' mitosis involving nuclear envelope breakdown (Burke and Ellenberg, 2002), the condensation of chromatin into mitotic chromosomes (Swedlow and Hirano, 2003), and the disruption of subnuclear compartments such as the nucleolus (Hernandez-Verdun et al., 2002; Leung and Lamond, 2003). Although the mechanisms of mitotic entry and exit have been well characterised, the re-establishment of chromosomal domains and subnuclear compartments including promyelocytic leukaemia (PML) nuclear bodies and nuclear organisation following mitosis has only just begun to be studied.

PML nuclear bodies have been implicated in a host of cellular processes including gene transcription (Ching et al., 2005; Zhong et al., 2000), viral pathogenicity (Everett, 2001; Regad and Chelbi-Alix, 2001), tumour suppression and cellular senescence (Salomoni and Pandolfi, 2002), apoptosis (Salomoni and Pandolfi, 2002) and DNA repair (Dellaire and Bazett-Jones, 2004). Although PML nuclear bodies do not contain nucleic acid in their protein-based core (Boisvert et al., 2000), they do make extensive contact with the surrounding chromatin and these contacts are responsible for both the structural integrity and limited mobility of PML

nuclear bodies during interphase (Eskiw et al., 2004; Eskiw et al., 2003).

It has been shown that the number and biochemistry of PML nuclear bodies change during the cell cycle. As cells progress from G1 to G2 the number of PML nuclear bodies increases (Koken et al., 1995; Terris et al., 1995). During S phase, the structural stability of PML nuclear bodies is altered such that a body undergoes several fission and fusion events, which together lead to a net increase in PML nuclear body number by a factor of up to twofold (Dellaire et al., 2006). However, this structural instability is not due to the loss of chromatin contacts. Rather, PML redistributes from a sphere surrounded by chromatin contacts to a distribution along a localised set of chromatin fibres. We proposed that during DNA replication, retraction of chromatin on the periphery, through topological changes, pulls PML out of the bodies. The resulting PML accumulations along the chromatin fibres maintain associations with the other PML nuclear body proteins, thus maintaining a biochemical composition indistinguishable from that of the parental bodies. Thus, PML nuclear body structure depends on contacts with chromatin as well as the integrity of chromatin itself (Dellaire et al., 2006; Eskiw et al., 2004). This led us to ask what is the fate of PML nuclear bodies as chromatin condenses and cells enter mitosis? Moreover, where is PML

found relative to chromatin during mitosis and how are new PML nuclear bodies formed in late mitosis/early G1?

It has been previously reported that the PML nuclear body number undergoes a dramatic decrease during mitosis (Stuurman et al., 1992; Koken et al., 1995; Terris et al., 1995). During late S phase Daxx translocates from PML nuclear bodies to sites of heterochromatin (Ishov et al., 2004), and in mitosis, PML nuclear bodies become depleted in Sp100 and SUMO-1 concomitantly with a reported hyperphosphorylation of the PML protein (Sternsdorf et al., 1997; Everett et al., 1999). As cells leave mitosis and re-enter G1, PML nuclear bodies contain both Sp100 and SUMO-1 (Everett et al., 1999). In this study, we extend these previous studies by providing high temporal resolution in the biochemical and morphological changes in PML nuclear bodies through mitosis. Specifically, we observe large mitotic accumulations of PML protein (MAPPs). Some of these are immobile, possibly through stable physical contacts with mitotic chromosomes. We also show that the mechanism of new PML nuclear body formation is based on the redistribution of PML from MAPPs, and protein synthesis of new PML is not required for the formation of PML nuclear bodies in early G1. We discuss these findings in the context of the role of PML nuclear bodies in the organisation of functional chromosomal domains in interphase nuclei.

## Results

**PML accumulations in mitosis do not behave as PML nuclear bodies: mobility and exchange of PML are altered**

In interphase, PML nuclear bodies are relatively immobile owing to extensive contacts with chromatin (Eskiw et al., 2004; Eskiw et al., 2003). When these chromatin contacts are disrupted by addition of transcriptional inhibitors such as actinomycin D or nucleases, PML nuclear bodies become fragmented and show increased mobility (Eskiw et al., 2004). Moreover, during early S phase, when euchromatin is replicated and major topological changes in the DNA occur, PML nuclear bodies become structurally unstable, leading to a 1.3- to 2-fold increase in number, through a series of fission and fusion events (Dellaire et al., 2006). We therefore asked whether PML nuclear body stability would be affected as chromatin condensation proceeds in early mitosis.

As previously shown we observe that the number of PML nuclear bodies changes during interphase (Stuurman et al., 1992; Koken et al., 1995; Everett et al., 1999). We observed an increase in HeLa cells from  $11 \pm 3$  nuclear bodies in G1 to  $23 \pm 7$  nuclear bodies in G2, presumably through fission of bodies in S phase (Dellaire et al., 2006). Instead of further structural instability and fission of parental bodies as chromatin begins to condense in prophase, as expected from our previous work, the number of PML nuclear bodies decreased to  $14 \pm 6$  nuclear bodies in mitosis, which is in agreement with earlier observations of PML nuclear body number in mitotic cells (Stuurman et al., 1992). Although the absolute number of PML nuclear bodies differs between cell types, this cell-cycle-dependent fluctuation in number occurred in all mammalian cell lines tested, including murine embryonic fibroblasts, normal diploid human fibroblasts (GM05757), SK-N-SH and U-2 OS (data not shown). To gain more insight into the mechanism for the decrease in PML nuclear body number in mitosis and to observe the changes with high temporal

resolution, we chose to examine live cells expressing GFP-PML. U-2 OS cells expressing GFP-PML IV were grown on coverslips and mitotic cells were located via differential interference contrast (DIC) microscopy. Single focal plane fluorescence images were collected initially every 4 minutes (Fig. 1A; Movie 1 in supplementary material) and then for higher temporal resolution, every 20 seconds (Fig. 1B). We directly observed the aggregation of PML nuclear bodies into larger PML accumulations as cells enter mitosis (Fig. 1A,B; Movie 2 in supplementary material). Although we observed that many of the PML accumulations were mobile in all three dimensions with respect to the focal plane (Fig. 1B, arrow; Fig. 1C, PML nuclear body 1), a subset of these structures also appeared to be relatively immobile and remained in focus for extended periods of time (Fig. 1B, arrowhead; Fig. 1C, PML nuclear bodies 2-4). Single particle tracking provided further evidence of populations of relatively immobile (Fig. 1C, nuclear body 1) and mobile (Fig. 1C, nuclear bodies 2-4) PML aggregates during mitosis. These observations indicate that although the majority of the PML mitotic accumulations are mobile, a subset may remain immobile by tethering to other cellular structures during mitosis.

We then asked whether PML protein exchanges with these structures as it does with PML nuclear bodies during interphase (Wiesmeijer et al., 2002). To address this, we located live interphase and mitotic U2OS cells expressing GFP-PML IV via DIC and imaged them by confocal fluorescence microscopy. A single PML nuclear body or mitotic accumulation of PML protein was then selected and bleached for fluorescence recovery after photobleaching (FRAP) analysis (Fig. 1D; Movie 3 in supplementary material). Images were collected at 1-minute intervals for 9 minutes following the bleach, and the fluorescence of each structure was monitored. The results of several FRAP experiments were averaged and the data plotted (Fig. 1D). In contrast to PML nuclear bodies in interphase cells, which undergo rapid exchange of PML protein, mitotic accumulations of PML protein did not readily undergo protein exchange and exhibited insignificant recovery after photobleaching (Fig. 1D; Movie 3 in supplementary material). Only minor fluorescence bleaching occurred (~5% of initial fluorescence) during imaging as demonstrated by the mean fluorescence intensity of unbleached PML nuclear bodies from interphase cells in the same field of view (Fig. 1D, control). Although the majority of the supramolecular accumulations of PML protein in mitosis are mobile, they do not dynamically exchange protein.

**The biochemical composition of mitotic accumulations of PML differs from PML nuclear bodies**

Because many of the PML accumulations become mobile and aggregate into large complexes, and because the exchange of PML protein itself differs from that observed in interphase, we expected that the biochemical composition of these mitotic PML accumulations also differs from interphase PML nuclear bodies. It has been shown that Sp100 becomes depleted from PML nuclear bodies as cells enter prophase (Sternsdorf et al., 1997; Everett et al., 1999) and that Daxx relocates from PML nuclear bodies to heterochromatin in late S phase (Ishov et al., 2004). The aim of these previous studies was not to provide the temporal resolution required to describe the biochemical and structural changes in PML nuclear bodies at all stages of

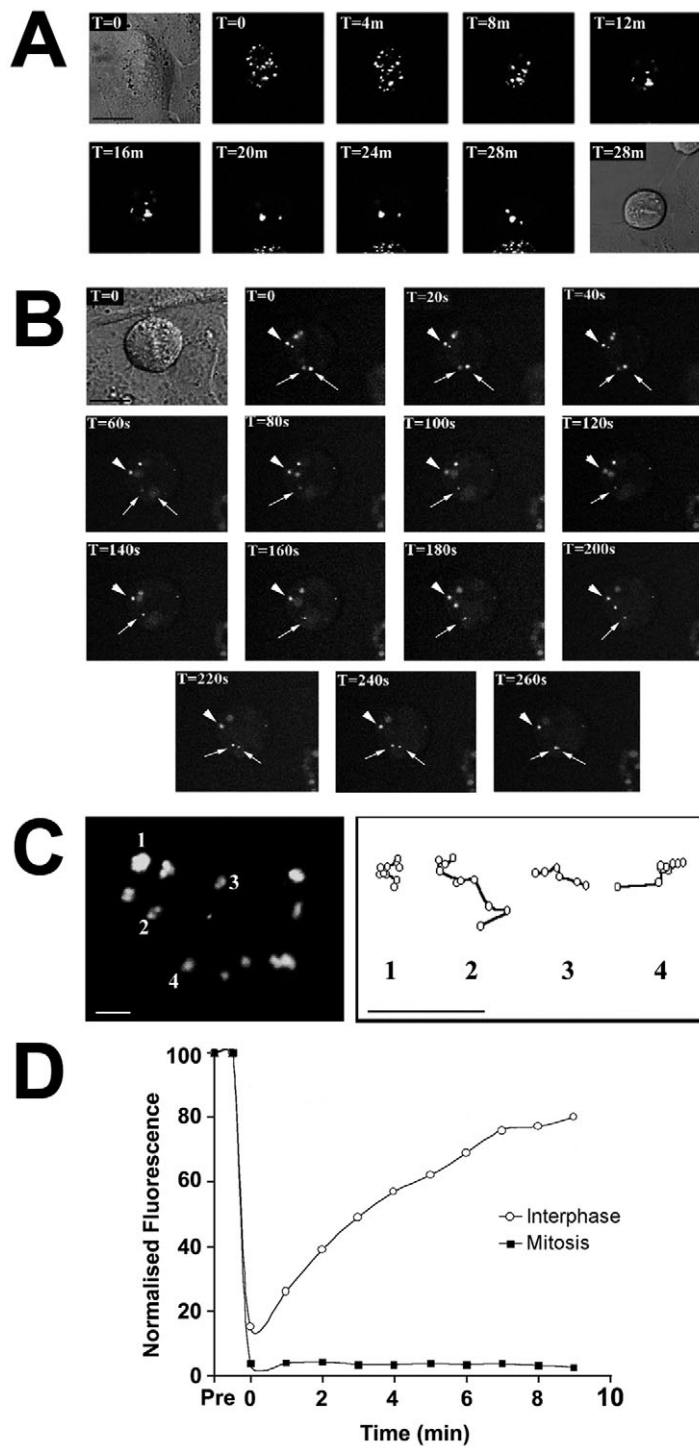


**Fig. 1.** Mobility of MAPPs during mitosis. Live U-2 OS cells stably expressing GFP-PML IV were imaged for the movement of MAPPs by DIC and fluorescence microscopy. (A) A cell in late G2 was followed into mitosis and fluorescence and DIC images were taken every 4 minutes (see Movie 1 in supplementary material). (B) A cell in mitosis was imaged by fluorescence and DIC microscopy and images were collected every 20 seconds. An initial DIC image is shown for  $t=0$ . Mobile MAPPs are indicated with arrows and relatively immobile MAPPs are indicated by arrowheads. (C) Single particle tracks of MAPPs in mitosis. The left panel shows a single frame of the movie of a mitotic cell in which several MAPPs (numbered 1-4) were tracked over time at 20 second intervals for 3 minutes. The relative position of each MAPP, corrected for cellular movement, was noted in each frame and plotted in the right panel. (D) PML protein dynamics in PML nuclear bodies in interphase and in MAPPs during mitosis. A single GFP-PML containing body or MAPP, respectively, was selected for FRAP analysis. An initial image was collected before a PML nuclear body (interphase, open circle) or MAPP (mitosis, closed square) was selected for bleaching. The selected PML nuclear body or MAPPs was then bleached and images collected every minute for 9 minutes. The intensity of the region of interest was normalised to the change in fluorescence intensity of the control, unbleached PML nuclear body, and expressed as a percent of the initial fluorescence (not shown). Several experiments were averaged (interphase  $n=20$ ; mitosis  $n=13$ ) and the mean percentage of fluorescence recovery was plotted over time in minutes. Bars, 5  $\mu\text{m}$  (A,B); 1  $\mu\text{m}$  (C).

In G1, the majority of PML nuclear bodies contained both Daxx (90%) and Sp100 (84%) (Table 1), which is consistent with the G1 accumulation of Sp100 in PML nuclear bodies described previously (Everett et al., 1999). The number of PML nuclear bodies containing Sp100 rose to 97% in G2 but was accompanied by a dramatic drop in the number of bodies containing Daxx (20%). In prophase the opposite trend occurred, where the number of PML nuclear bodies containing Sp100 decreased to 87% and the number of bodies containing Daxx actually increased to 47%. As cells progressed from prophase into metaphase the lamin A/C signal appeared at first punctate, as nuclear envelope integrity was compromised, followed by a progressive loss of lamin A/C signal at the nuclear periphery that correlated with the loss of Sp100 from PML nuclear bodies (Fig. S2 in supplementary material). During this time PML nuclear bodies appeared to remain intact, which is in sharp contrast to the disruption of PML nuclear bodies seen when chromatin is prematurely condensed by heat shock or the inhibition of transcription (Eskiw et al., 2004; Eskiw et al., 2003). By prometaphase only 2% of PML nuclear bodies were enriched in Sp100 above background, and Daxx could not be detected in these bodies above background (Table 1). In addition to Sp100 and Daxx, we also observed the concomitant reduction of SUMO-1 levels as cells progressed from prophase to metaphase (data not shown), agreeing with previous studies (Everett et al., 1999). By metaphase, the majority of PML nuclear bodies do not contain Sp100, Daxx or SUMO-1 and the bodies appear to form large aggregates (Figs S1 and S2 in supplementary material). As the nuclear envelope breaks down, the biochemical composition of the bodies changes dramatically, evidenced by the loss of Sp100, Daxx and SUMO-1, correlating with major differences in their dynamic

mitosis. Therefore we sought to determine the precise temporal changes in PML nuclear body biochemistry from G2, through the stages of mitosis, and into early G1. To accomplish this, unsynchronised HeLa cells were fixed and processed for the immunodetection of PML, Sp100 and Daxx simultaneous with detection of phosphorylated histone H3 (to monitor cells in G2) (Hendzel et al., 1997) and lamin A/C (to identify cells in prophase to prometaphase) (Burke and Ellenberg, 2002). DAPI was used to visualise chromatin at various stages of the cell cycle (Figs S1 and S2 in supplementary material).



**Table 1. Percentage of PML nuclear bodies or MAPPs associated with Sp100 or Daxx during the cell cycle**

	G1	G2	Prophase	Prometaphase	Metaphase	Anaphase	Telophase	Early G1
Sp100	84	97	83	2	0	0	9	26
Daxx	90	20	47	0	0	0	0	9

behaviour compared with interphase PML nuclear bodies. Since both the composition and dynamic properties are so different from interphase PML nuclear bodies, we refer to these structures from here on as mitotic accumulations of PML protein (MAPPs) rather than as mitotic PML bodies.

By anaphase, the MAPPs were completely devoid of Sp100 and Daxx (Figs S1 and S2 in supplementary material). Although re-formation of the nuclear envelope was evident in telophase, nuclear envelope formation was not complete and PML nuclear bodies within the nascent nuclei had not yet been re-established. In telophase only 9% of MAPPs contained Sp100, and Daxx could not be detected in these structures (Table 1). As nuclear envelope re-formation was nearing completion at cytokinesis/early G1, PML nuclear bodies were present in the nucleoplasm of both daughter nuclei and had begun to accumulate both Sp100 and Daxx. The temporal resolution of this study allowed us to observe that Daxx accumulates more slowly in PML nuclear bodies than Sp100 in early G1 (9% compared with 26% of PML nuclear bodies, respectively) (Table 1). The differential accumulation of Daxx and Sp100 may represent a specific temporal order of PML nuclear body reassembly. These data also demonstrated a clear correlation between the biochemical integrity of PML nuclear bodies and an intact nuclear envelope.

#### A subset of MAPPs remain associated with mitotic chromosomes providing a potential mechanism for segregation of PML protein during mitosis

It was possible that the immobile subset of MAPPs observed in mitotic cells could be tethered to chromosomes, thereby providing a mechanism for PML protein to become incorporated into newly forming daughter nuclei. In agreement with this hypothesis, we observed MAPPs in mitotic cells that appeared to be in close contact with the chromosomes by immunofluorescence detection of PML (Fig. S2A in supplementary material, white arrowhead). To further characterise the association of these MAPPs with chromosomes, we compared the number of MAPPs associated with mitotic chromosomes in HeLa cells grown on coverslips in metaphase/anaphase with MAPPs associated with chromosomal spreads prepared by the cytopsin technique (Fig. 2A,B). The mean number of MAPPs in mitotic HeLa cells prepared by cytopsin was  $4 \pm 2$  versus  $30 \pm 5$  in mitotic cells visualised on coverslips (Table 2). The cytopsin procedure involves detergent extraction and is

commonly used to observe tightly associated chromosomal proteins such as those at the centromere (e.g. CENPA, B, C and H) (Sugata et al., 2000). The fact that this technique extracted more than 85% of the MAPPs suggests strongly that association of these structures with chromatin is not an artefact of precipitation of PML protein during cytopsin. The subset of MAPPs found tightly associated with condensed chromosomes after the cytopsin procedure was  $3 \pm 2$  or 75% of the total MAPPs, compared with  $6 \pm 3$  or 20% of the total MAPPs in a mitotic cell on a coverslip (Fig. 2A,B, white arrowheads). These data may indicate that there are as few as three very high affinity chromosomal binding sites for PML complexes during mitosis in HeLa cells.

To provide further evidence for a physical interaction between MAPPs and mitotic chromosomes we analysed this association at the ultrastructural level (Fig. 2C-F). Asynchronous cells were labelled with anti-PML and anti-phospho H3 (Ser10) antibodies. Phospho-H3 labelling is used as a marker for easy recognition of late G2-mitotic cells via fluorescence microscopy. Labelled cells were embedded in plastic resin and physical sections of 70 nm were prepared by ultramicrotomy. These physical sections were collected on grids and analysed by fluorescence microscopy. Within the regions indicated, PML protein (yellow) appeared to be associated with mitotic chromosomes (blue) (Fig. 2C). Electron spectroscopic imaging (ESI) (Dellaire et al., 2004) of physical sections revealed accumulations of PML protein in contact with mitotic chromosomes (Fig. 2E,F, white arrowhead). These PML accumulations lacked the characteristic radial symmetry and ring morphology of PML bodies observed in G1-G2 nuclei (Maul, 1998; Lallemand-Breitenbach et al., 2001; Eskiw et al., 2003). Later in mitosis and into late cytokinesis, MAPPs can be seen associated with decondensing chromatin and can be 'trapped' within the newly forming nucleus, often before re-formation of the nuclear envelope is complete (Fig. 2G). These data indicate that a subset of MAPPs can accompany mitotic chromosomes during mitosis, providing a mechanism by which PML nuclear bodies are potentially formed in daughter nuclei.

#### MAPPs contribute to the post-mitotic formation of PML nuclear bodies: a process that does not require new protein synthesis

Although PML nuclear bodies rapidly form within the nucleus of each daughter cell following mitosis, we observed that there was a large portion of the total PML protein that remained in the cytoplasm during G1 in the form of MAPPs (Figs S1 and S2 in supplementary material). In mitosis, these cytoplasmic MAPPs do not contain detectable levels of PML nuclear body components such as Sp100 or Daxx and are, therefore, biochemically distinct from PML nuclear bodies (Figs S1 and S2 in supplementary material). In addition, they do not exchange PML protein and thus appear to be inert aggregates of protein (Fig. 1D). However, in G1 cells we observed that the number of MAPPs decreased over time. Therefore, we wished

**Table 2. Quantification of MAPPs associated with chromosomes in mitotic cells**

	Total MAPPs*	Chromosome associated MAPPs (%) <sup>†</sup>
Coverslip	$30 \pm 5$	$6 \pm 3$ (20)
Cytopsin	$4 \pm 2$	$3 \pm 2$ (75)

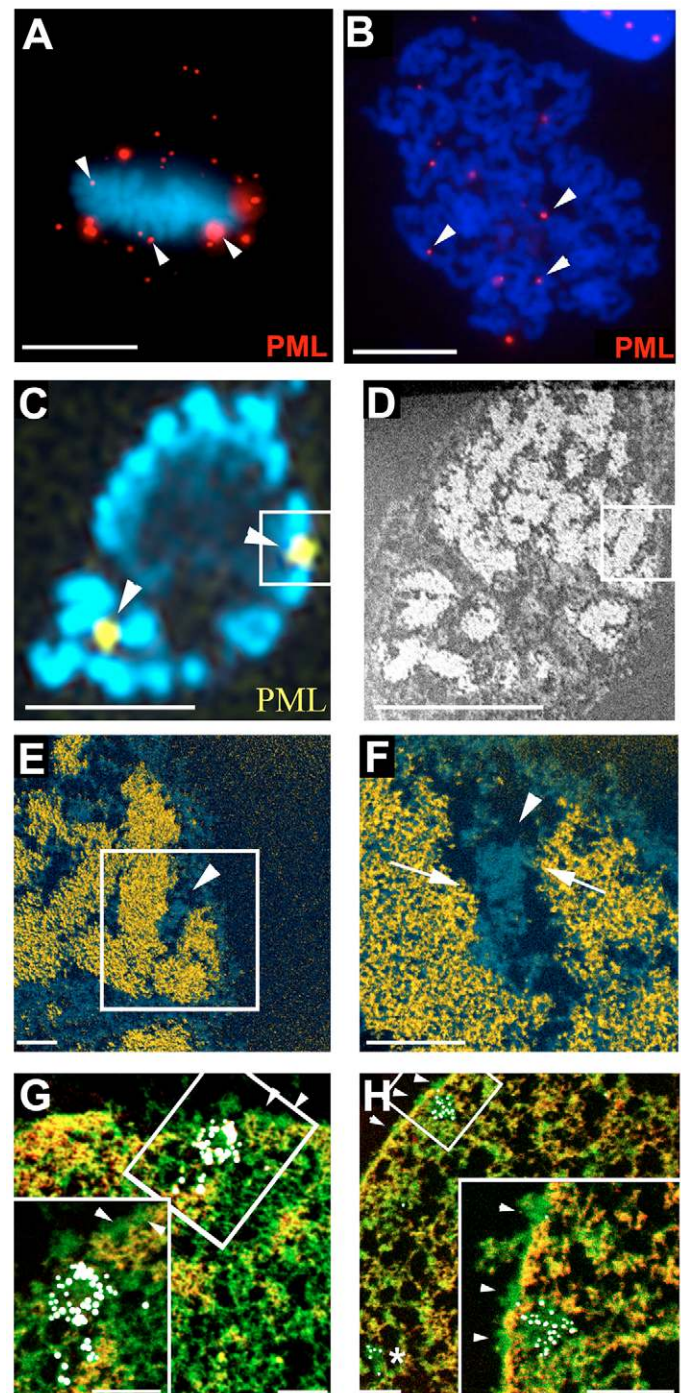
\*Mean body number  $\pm$  s.d. <sup>†</sup>Percentage is based on mean number of MAPPs.

to determine the reason for the observed disappearance of MAPPs in G1 cells.

The observed loss of cytoplasmic MAPPs in G1 cells could be due to the degradation of PML protein by the 26S proteasome pathway (Hartmann-Petersen et al., 2003). To test if this pathway was involved in degrading PML, HeLa cells were treated with nocodazole and analysed following mitotic shake-off in the presence or absence of the 26S proteasome inhibitor MG132 (Fig. 3). After shake-off and drug treatment, cells were allowed to adhere to slides before being fixed and labelled for PML protein at 2 hour intervals. As cells left mitosis and progressed through G1, we observed fewer cells containing MAPPs in both control and MG132-treated cells (Fig. 3A). There was no statistical difference in the number of cells containing MAPPs for each interval between the control and MG132 treatments (Fig. 3B). Therefore, degradation of PML protein by the 26S proteasome pathway does not explain the disappearance of MAPPs from the cytoplasm of G1 cells.

**Fig. 2.** Localisation of PML-containing structures in human cells during mitosis and early G1 by light and electron microscopy. (A,B) Immunolocalisation of mitotic accumulations of PML protein (MAPPs) (red) in a mitotic HeLa cell grown on a coverslip (A) or a HeLa mitotic spread prepared by cytospin (B). White arrowheads indicate examples of MAPPs closely associated with chromosomes. DNA is counterstained with DAPI (blue). Note that the image shown in panel B is of two overlapping mitotic spreads. (C-F) Correlative light and electron microscopy of MAPPs associated with mitotic chromosomes. Mitotic HeLa cells were shaken from flasks and plated on coverslips before processing for correlative light and ESI. (C) A correlative fluorescence image of an ultra thin section (70 nm) of a mitotic SK-N-SH cell grown on a coverslip is shown labelled for PML (yellow) and phospho-H3 (blue). This image was used to correlate the location of MAPPs (yellow) in the electron micrograph in D. (D) Low magnification electron micrograph (155 keV phosphorus-enriched) of the mitotic cell in C. (E) Composite electron micrograph of nitrogen and phosphorus maps collected by ESI, which details the protein-based structures (blue) and chromatin (yellow) of the mitotic cell. The white arrowhead indicates the MAPP seen in B. A white box indicates the area of interest containing a MAPP to be imaged at higher magnification. (F) Higher magnification composite ESI micrograph of the MAPP within the white box indicated in panel E. Small white arrows indicate positions where the MAPP (blue structure, white arrowhead) makes direct contact with chromatin (yellow). (G,H) PML nuclear bodies form in early G1 nuclei by entrapment of MAPPs and/or nuclear import of PML protein. Asynchronous HeLa cells were fixed and processed for the immunogold detection of PML by ESI. (G) An ESI micrograph of a HeLa cell in late cytokinesis is shown. In this micrograph a PML accumulation appears to have been entrapped by the reforming nuclear envelope, as indicated by a cluster of immunogold labelling for the PML protein (white dots). A region of interest containing this nascent PML nuclear body (defined by the white square), is shown as an inset. The arrowheads indicate nuclear pore, though the region to the left of the arrowheads, close to the MAPP where the nuclear envelope has not completely re-formed. (H) An ESI micrograph of a HeLa cell in early G1 is shown in which two PML nuclear bodies can be seen, one near the nuclear envelope (defined by the white box; shown at higher magnification in the inset) and a smaller PML nuclear body in the lower left corner of the micrograph (white asterisk). Two nucleopores are shown associated with immunogold complexes directed against PML (inset). Bars, 10  $\mu\text{m}$  (A,B); 5  $\mu\text{m}$  (C,D); 1  $\mu\text{m}$  (E,F); 0.5  $\mu\text{m}$  (G,H).

The failure of the 26S proteasome inhibitor MG132 to prevent the loss of MAPPs during G1 led us to the hypothesis that PML protein may be recycled from one cell cycle to the next via MAPPs, similarly to the fate of pre-mRNA splicing factors within mitotic interchromatin granules (MIGs) (Prasanth et al., 2003). To test this hypothesis, HeLa cells were analysed after mitotic shake-off in the presence or absence of the protein synthesis inhibitor cycloheximide. Since no new protein is translated in cycloheximide-treated cells, PML nuclear body formation after cytokinesis would depend solely on PML nuclear body components from the previous cell cycle. PML nuclear bodies were observed in the daughter nuclei of





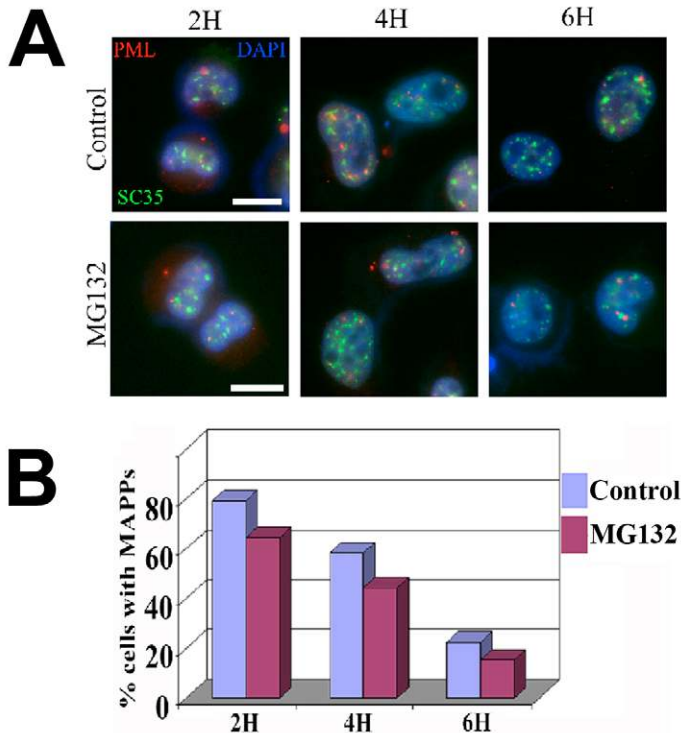


**Fig. 3.** PML protein within MAPPs is not degraded by the 26S proteasome pathway during mitosis. (A) Mitotic HeLa cells were prepared by shake-off from an asynchronous population and plated on coverslips in medium containing 20 mM MG132 and allowed to grow for 2 hours (2H), 4 hours (4H) and 6 hours (6H). Cells were then fixed, processed for the immunodetection of PML (red), SC35 (green) and DNA was counterstained with DAPI. (B) The proteasome does not contribute to the loss of MAPPs in G1 nuclei. The percentage of cells containing PML nuclear bodies was similar between control (blue) and MG132 treated (purple) HeLa cells and no statistical difference was observed for the number of bodies per cell (data not shown). DNA was counterstained with DAPI (blue). Bar, 5  $\mu$ m.

G1 cells, containing the full complement of typical PML nuclear body components, such as Sp100 (data not shown). In addition, we observed no significant difference between the number of PML nuclear bodies per cell between control and cycloheximide-treated cells (data not shown). Thus, de novo protein synthesis is not required for PML nuclear body formation in G1.

Although we have demonstrated that PML protein is recycled from one cell cycle to the next, it was unclear how MAPPs were incorporated into nuclei after the re-formation of the nuclear membrane. One possibility is that MAPPs are dissociated into molecular PML or macromolecular PML-containing complexes, which enter daughter nuclei by transport across the nuclear envelope via the nuclear pore complex. To address this possibility, unsynchronised HeLa cells were processed for the immunogold detection of PML and analysis by ESI (Fig. 2G,H). Correlative microscopy was used to locate PML containing structures within G1 nuclei and these were imaged using ESI. PML protein labelled with gold can be seen in the vicinity of nuclear pores as well as within the pore complexes themselves, indicating that PML protein is

being transported between the cytoplasm and nucleus via the nuclear pores (Fig. 2H). It is formally possible that the PML observed in the pores could be moving from the nucleus to the cytoplasm. However, because there is a net increase of PML in the nucleus and a net decrease of PML in the cytoplasm during this time period, we conclude that the majority of the PML observed in the pores is probably moving into the nucleus. The observations of entrapped MAPPs in newly forming nuclei (Fig. 2G), and PML passing through nuclear pores (Fig. 2H), were not unique to HeLa cells, because we observed these events in other cells types, including SK-N-SH neuroblastoma cells (data not shown).

## Discussion

We and others have demonstrated that the number, integrity and biochemistry of PML nuclear bodies continually change during the cell cycle (Stuurman et al., 1992; Koken et al., 1995; Terris et al., 1995; Sternsdorf et al., 1997; Everett et al., 1999; Ishov et al., 2004; Dellaire et al., 2006). In the present study, we extend these observations to the comparative analysis of Daxx and Sp100 during the cell cycle (Table 1; Figs S1 and S2 in supplementary material). Daxx has been shown to accumulate at sites of heterochromatin in late S phase in murine fibroblasts, and in the absence of Daxx, S-phase progression is accelerated (Ishov et al., 2004), suggesting that Daxx may have a function outside of the body in late S phase. This is consistent with our observation here that all PML nuclear bodies contain Sp100 in G2, but only 20% contain Daxx. Similarly, as daughter cells progress through early G1, Sp100 precedes the recruitment of Daxx back to PML nuclear bodies. The functional significance of the differential accumulation of other PML nuclear body components during the cell cycle, including Sp100, remains to be addressed. In this study, we have also correlated the loss of these biochemical markers of interphase PML nuclear bodies, with the dynamics of both molecular and supramolecular PML in the form of mitotic accumulations of PML protein (MAPPs). We provide the first evidence that PML protein is recycled from one cell cycle to the next via MAPPs and evidence for at least two mechanisms by which these structures contribute to the formation of PML nuclear bodies in G1, as discussed below.

As cells enter mitosis, the PML nuclear body number drops by the aggregation of these bodies into larger MAPPs (Fig. 1, Movie 2 in supplementary material). This aggregation correlates with both the loss of nuclear envelope integrity and the loss of Daxx, Sp100 and SUMO-1 (Figs S1 and S2 in supplementary material). Although the MAPPs are highly mobile (Fig. 1A-C), they do not readily exchange PML protein and they appear to aggregate, i.e. remaining as discrete structures though contacting each other, rather than fusing into single spheres (Fig. 1D; Movie 3 in supplementary material). As cells exit mitosis, progressing through cytokinesis and entry into early G1, MAPPs persist for several hours in the cytoplasm while PML nuclear bodies begin to form in each daughter nucleus (Everett et al., 1999). Thus, MAPPs appear to provide a source of PML to the daughter nuclei. This is analogous to the apparent function of MIGs, which provide a source of nuclear speckle components during the re-formation of nuclear speckles in daughter nuclei (Prasanth et al., 2003). Two major differences, however, distinguish MAPPs and MIGs. Whereas most PML nuclear-body-associated proteins dissociate from PML in mitosis, many nuclear speckle components remain

associated with MIGs during mitosis. Second, MAPPs persist for a long time in the cytoplasm of G1 cells, whereas MIGs rapidly disappear as cells progress through anaphase (Prasanth et al., 2003) (Fig. S3 in supplementary material). In addition, we show that MIGs (labelled by SC35) and MAPPs are spatially and biochemically distinct and the re-formation of PML nuclear bodies and interchromatin granule clusters (IGCs) from their respective cytoplasmic accumulations do not appear to be co-regulated because these events are temporally separate (Fig. S3 in supplementary material).

Although PML protein synthesis is elevated in G1 cells (Dellaire et al., 2006; Chang et al., 1995), we have demonstrated that the post-mitotic re-establishment of PML nuclear bodies can proceed without de novo protein synthesis via at least two mechanisms. The first mechanism involves the association of MAPPs with mitotic chromosomes. We observed a subset of MAPPs that were relatively immobile, probably through physical contact with mitotic chromosomes. Chromosome-associated MAPPs are then entrapped by the reformation of the nuclear envelope in late telophase/cytokinesis (Fig. 2G), and thus provide both a source of PML protein as well as a potential mechanism for the initial stages of PML nuclear body formation in early G1 nuclei. The association of PML protein in the form of MAPPs with mitotic chromosomes is not a newly discovered mechanism by which components of nuclear compartments are incorporated into daughter nuclei. For example, upstream binding factor (UBF) associates with nucleolar organising regions and marks this chromatin as the future sites of nucleoli formation (Roussel et al., 1996; Roussel et al., 1993). Therefore, association of a subset of nuclear compartment proteins with mitotic chromosomes may function as a common mechanism to seed the formation of these structures in the next cell cycle.

The second mechanism of PML nuclear body formation in G1, involves the redistribution of PML protein from cytoplasmic MAPPs to the site of PML nuclear bodies. These structures decreased in number over time and we demonstrated that the 26S proteasome pathway does not degrade cytoplasmic MAPPs (Fig. 3). We also demonstrated that in the absence of de novo protein synthesis, PML nuclear bodies were able to reform in early G1 cells. The loss of MAPPs from the cytoplasm and the increase in PML nuclear body numbers indicated that PML protein from the MAPPs was being incorporated into PML nuclear bodies within daughter nuclei. Finally ESI micrographs indicated that PML protein can pass through the nuclear pore complexes to sites of new PML nuclear body formation in early G1 (Fig. 2G,H).

These two mechanisms for the post-mitotic re-establishment of PML nuclear bodies formation need not be mutually exclusive and it is conceivable that chromosome-associated MAPPs provide the seed from which PML nuclear bodies grow through the redistribution of PML protein from cytoplasmic MAPPs. Our observation that supramolecular PML structures remain associated with mitotic chromosomes is particularly interesting in light of recent evidence that PML nuclear bodies are non-randomly associated with transcriptionally active, gene-rich chromosomal regions (Wang et al., 2004), including the MHC class I gene cluster on human chromosome 6 (Shiels et al., 2001). Not all PML nuclear bodies are necessarily associated with transcriptionally active gene loci. We have observed a subset of morphologically distinct PML nuclear

bodies at the edges of heterochromatin associated with the nucleolus (our unpublished observations). Some PML nuclear bodies in telomerase-negative cells are associated with transcriptionally inert telomeric DNA (Grobelny et al., 2000; Yeager et al., 1999), and heritable positioning of PML nuclear bodies in relation to HSV-1 replication foci in early G1 has also been reported (de Bruyn Kops and Knipe, 1994; Maul, 1998). Therefore, it is tempting to speculate that the chromosome-attached MAPPs observed in mitosis seed the formation of PML nuclear bodies at specific gene loci in G1. A corollary to this hypothesis is that PML nuclear body formation with respect to chromosomal loci is not only non-random but is heritably transmitted through mitosis. We are currently testing this hypothesis.

In contrast to any other time in the cell cycle, a substantial fraction of PML protein is found in the cytoplasm in early G1 (Sternsdorf et al., 1997; Everett et al., 1999) (Figs S1 and S2 in supplementary material). One interpretation is that these cytoplasmic accumulations are simply storage sites for the recycling of PML by nuclear import into new PML nuclear bodies. However, it appears that at least some isoforms of the PML protein, may exist in the cytoplasm under certain conditions where they carry out specific function(s) (Borden, 2002; Lin et al., 2004). PML can act as a translational repressor by reducing the affinity of eIF4E translation factor for the m<sup>7</sup>G cap of processed mRNAs and occluding the binding of eIF4G to eIF4E (Kentsis et al., 2001). Therefore, MAPPs may play a role in translational repression during early G1. However, we have been unable to demonstrate any appreciable accumulation of eIF4E over background within PML nuclear bodies in interphase cells or in MAPPs during mitosis (data not shown). The PML protein may still function in translational repression through eIF4E but we have no evidence to suggest MAPPs play a role in this process. A recent study by Pandolfi and colleagues also suggests a broader function for cytoplasmic isoforms of PML in regulating TGF- $\beta$  signaling, which implicates PML through yet another pathway of tumour suppression (Lin et al., 2004). The localisation of these endogenous PML isoforms during the cell cycle, however, was not addressed. Although several studies provide compelling evidence for a role for cytoplasmic accumulations of PML beyond storage, it is not clear whether PML persists in the cytoplasm in any appreciable amount at other times in the cell cycle outside early G1.

The maintenance of nuclear compartments such as nuclear speckles and PML nuclear bodies by the recycling of their components from one cell cycle to the next provides a paradigm that may be useful for the study of other nuclear compartments. Only by understanding how these functional compartments are re-established in each cell cycle will we fully comprehend how chromosomes and the individual genes within them are organised and regulated within the interphase nucleus.

## Materials and Methods

### Cell Culture, mitotic shake-off assays and chromosomal preparations

HeLa cells (American Type Tissue Culture Collection) were cultured in Dulbecco's modified Eagle's medium supplemented with 10% fetal bovine serum (FBS; Sigma) and U-2 OS cells stably expressing GFP-PML IV (a generous gift from J. Taylor, University of Wisconsin, Madison, WI) were cultured in growth medium supplemented with 1600  $\mu$ g/ml G418 (Wisent). For mitotic shake-off

assays, cells were grown between 18 and 20 hours in media containing 50 ng/ml nocodazole (Calbiochem). Coverslips for shake-off assays were prepared by incubation with 0.1% poly-lysine (Sigma) in PBS for 10 minutes. Cells were treated with 20 mM MG132 (Calbiochem) in growth medium to inhibit 26S proteasomal degradation. Protein synthesis was inhibited by the addition of 150 µg/ml cycloheximide (Sigma) to culture medium, which inhibited protein translation in HeLa cells by over 90% as determined by [<sup>3</sup>H]leucine incorporation, as previously described (Williams et al., 1999). Chromosomal preparations were from HeLa cells resuspended in hypotonic buffer (33.5 mM KCl, 17 mM trisodium citrate) at a concentration of 2×10<sup>5</sup> cells/ml. Cells were then deposited onto glass slides at 1900 rpm for 10 minutes using a Shandon Cytospin 4 (Thermo Electron). Slides were immediately removed and incubated in KCM buffer (10 mM Tris-HCl pH 7.7, 120 mM KCl, 20 mM NaCl, 0.1% Triton X-100) for 10 minutes at room temperature (RT) with or without prior fixation in 2% paraformaldehyde (PFA) (Electron Microscopy Sciences) in PBS at room temperature for 10 minutes. Slides were then subjected to immunofluorescence detection of proteins.

### Immunofluorescence detection of proteins, live-cell imaging and FRAP

Cells growing on coverslips were fixed for 5 minutes in 2% paraformaldehyde in PBS at RT. Cells were then permeabilised for 10 minutes in PBS/0.5% Triton X-100 at RT, followed by three 5 minute washes in PBS. Cytospin chromosome preparations were immunolabelled directly without fixation. Cells were immunolabelled with either rabbit anti-PML (1:1000) (Chemicon, AB1370), mouse anti-PML (1:5) (5E10, a gift from R. Van Driel, University of Amsterdam, The Netherlands), rabbit anti-Sp100 (1:500) (Chemicon, Ab1380), goat anti-Daxx (1:200) (Santa Cruz Biotech), mouse anti-GMP1 (1:20) (Zymed), rabbit anti-phospho H3 (1:200) (Upstate) or mouse anti-Lamin A/C (1:2) (a generous gift from B. Burk, University of Florida, Gainesville, FL). Cells were further labelled with secondary antibodies conjugated to Cy3 (1:500), Cy5 (1:100) or Alexa Fluor 488 (1:200) (Jackson ImmunoResearch Laboratories). DNA was stained with 4,6'-diamidino-2-phenylindole (DAPI) (Sigma) in mounting media containing 90% glycerol and 1 mg/ml paraphenylenediamine (PPDA) (Sigma). Immunogold labelling was accomplished using a secondary antibody (1:200) conjugated to ultra-small (0.8 nm) gold (EMS). Fluorescence micrographs of fixed cells were collected on a Leica DMR2 upright fluorescence microscope fitted with a Hamamatsu Orca camera. OpenLab 3.5.1 software (Improvision) was used for image acquisition. Live-cell imaging of the distribution of GFP-PML IV in U-2 OS cells during mitosis was carried out on unsynchronised cells as previously described (Eskiw et al., 2004), with the exception that cells were placed in RPMI medium (Wisent) supplemented with 10% FBS during imaging. FRAP experiments were conducted on a Zeiss LSM 510 confocal microscope equipped with an argon laser (488 nm). Entire PML-containing structures (i.e. MAPPs or nuclear bodies) in mitotic or interphase cells were bleached with 25% power and 100% transmittance of laser light. Projections were made of z-stacks of the bleached structures, imaged with the maximum pinhole diameter to minimise z-resolution, that were collected at 1 minute intervals. Because the structures were mobile, we defined a region of interest (ROI) in an appropriate z-slice at each time point. To visualise the bleached structure and define the region of interest, we expanded the display intensity of the FRAP signal. The ROIs of the equivalent slice from each time point were applied to the raw data to measure the fluorescence recovery. ImageJ version 1.30 (NIH) and Photoshop version 7.0 (Adobe) software were used for image processing.

### Quantitative analysis of PML nuclear body components and MAPPs associated with chromosomes in HeLa cells

PML nuclear bodies were counted in Z-projections of asynchronous HeLa cells immunolabelled for PML and Daxx or Sp100 as described above. G1 cells prepared by analysing HeLa cells 1-2 hours after mitotic shake-off and early-G1 nuclei, enriched at 0.5-1 hour post shake-off, are characterised predominately by accumulations of PML-containing structures outside of nuclei. Other phases of the cell cycle were determined by the morphology of the nuclear lamina and chromosomes and/or immunodetection of phospho-histone H3 (a G2 marker). PML nuclear bodies from 30 nuclei in each cell cycle phase were scored as having Sp100 or Daxx above background nucleoplasmic levels. The percentage of total bodies counted that contained either Sp100 or Daxx at various times in the cell cycle is presented in Table 1.

Mitotic cells grown on coverslips or prepared by cytospin were subjected to the immunofluorescence detection of PML as described above. MAPPs were then counted by scoring PML-containing structures in Z-projections of images taken at 0.5 µm intervals using Image J version 1.30 (NIH). The mean number of MAPPs per mitotic cell versus the mean number of MAPPs associated with chromosomes is presented in Table 2.

### Correlative microscopy and electron spectroscopic imaging

Samples were prepared and sectioned for correlative microscopy and ESI as previously described (Dellaire et al., 2004; Eskiw et al., 2003). Fluorescence images

of physical sections were collected on a Leica DMR2 fluorescence microscope as previously described (Dellaire et al., 2004), to allow the location of cells and structures of interest to be correlated between light and electron microscopy. Nitrogen and phosphorus maps were collected using an FEI Tecnai 20 transmission electron microscope fitted with an electron-imaging spectrometer (Gatan). Elemental maps were false coloured and merged using Adobe Photoshop version 7.0 (Adobe) software.

We thank Roel van Driel for the gift of the 5E10 PML monoclonal antibody and Jerry Taylor for providing U-2 OS cells expressing PML-IV. We also acknowledge the skilled work of Ren Li for aid in the preparation and imaging of serial sections for the ESI micrographs. G.D. is a Senior Postdoctoral Fellow of the Canadian Institutes of Health Research (CIHR), and both C.H.E. and R.W.C. are recipients of the Restrucamp Studentship from the Hospital for Sick Children Research Institute. D.P.B.-J. is a recipient of a Canada Research Chair in Molecular and Cellular Imaging. This research was supported by an operating grant (MOP-64405) from the CIHR.

### References

- Boisvert, F. M., Hendzel, M. J. and Bazett-Jones, D. P. (2000). Promyelocytic leukemia (PML) nuclear bodies are protein structures that do not accumulate RNA. *J. Cell Biol.* **148**, 283-292.
- Borden, K. L. (2002). Pondering the promyelocytic leukemia protein (PML) puzzle: possible functions for PML nuclear bodies. *Mol. Cell. Biol.* **22**, 5259-5269.
- Burke, B. and Ellenberg, J. (2002). Remodelling the walls of the nucleus. *Nat. Rev. Mol. Cell. Biol.* **3**, 487-497.
- Chang, K. S., Fan, Y. H., Andreoff, M., Liu, J. and Mu, Z. M. (1995). The PML gene encodes a phosphoprotein associated with the nuclear matrix. *Blood* **85**, 3646-3653.
- Ching, R. W., Dellaire, G., Eskiw, C. H. and Bazett-Jones, D. P. (2005). PML bodies: a meeting place for genomic loci? *J. Cell Sci.* **118**, 847-854.
- de Bruyn Kops, A. and Knipe, D. M. (1994). Preexisting nuclear architecture defines the intranuclear location of herpesvirus DNA replication structures. *J. Virol.* **68**, 3512-3526.
- Dellaire, G. and Bazett-Jones, D. P. (2004). PML nuclear bodies: dynamic sensors of DNA damage and cellular stress. *BioEssays* **26**, 963-977.
- Dellaire, G., Nisman, R. and Bazett-Jones, D. P. (2004). Correlative light and electron spectroscopic imaging of chromatin in situ. *Methods Enzymol.* **375**, 456-478.
- Dellaire, G., Ching, R. W., Dehghani, H., Ren, Y. and Bazett-Jones, D. P. (2006). The number of PML nuclear bodies increases in early S phase by a fission mechanism. *J. Cell Sci.* **119**, 1026-1033.
- Eskiw, C. H., Dellaire, G., Mymryk, J. S. and Bazett-Jones, D. P. (2003). Size, position and dynamic behavior of PML nuclear bodies following cell stress as a paradigm for supramolecular trafficking and assembly. *J. Cell Sci.* **116**, 4455-4466.
- Eskiw, C. H., Dellaire, G. and Bazett-Jones, D. P. (2004). Chromatin contributes to structural integrity of promyelocytic leukemia bodies through a SUMO-1-independent mechanism. *J. Biol. Chem.* **279**, 9577-9585.
- Everett, R. D. (2001). DNA viruses and viral proteins that interact with PML nuclear bodies. *Oncogene* **20**, 7266-7273.
- Everett, R. D., Lomonte, P., Sternsdorf, T., van Driel, R. and Orr, A. (1999). Cell cycle regulation of PML modification and ND10 composition. *J. Cell Sci.* **112**, 4581-4588.
- Grobely, J. V., Godwin, A. K. and Broccoli, D. (2000). ALT-associated PML bodies are present in viable cells and are enriched in cells in the G(2)/M phase of the cell cycle. *J. Cell Sci.* **113**, 4577-4585.
- Hartmann-Petersen, R., Seeger, M. and Gordon, C. (2003). Transferring substrates to the 26S proteasome. *Trends Biochem. Sci.* **28**, 26-31.
- Hendzel, M. J., Wei, Y., Mancini, M. A., Van Hooser, A., Ranalli, T., Brinkley, B. R., Bazett-Jones, D. P. and Allis, C. D. (1997). Mitosis-specific phosphorylation of histone H3 initiates primarily within pericentromeric heterochromatin during G2 and spreads in an ordered fashion coincident with mitotic chromosome condensation. *Chromosoma* **106**, 348-360.
- Hernandez-Verdun, D., Roussel, P. and Gebrane-Younes, J. (2002). Emerging concepts of nucleolar assembly. *J. Cell Sci.* **115**, 2265-2270.
- Ishov, A. M., Vladimirova, O. V. and Maul, G. G. (2004). Heterochromatin and ND10 are cell-cycle regulated and phosphorylation-dependent alternate nuclear sites of the transcription repressor Daxx and SWI/SNF protein ATRX. *J. Cell Sci.* **117**, 3807-3820.
- Kentsis, A., Dwyer, E. C., Perez, J. M., Sharma, M., Chen, A., Pan, Z. Q. and Borden, K. L. (2001). The RING domains of the promyelocytic leukemia protein PML and the arenaviral protein Z repress translation by directly inhibiting translation initiation factor eIF4E. *J. Mol. Biol.* **312**, 609-623.
- Koken, M. H., Linares-Cruz, G., Quignon, F., Viron, A., Chelbi-Alix, M. K., Sobczak-Thépot, J., Juhlin, L., Degos, L., Calvo, F. and de Thé, H. (1995). The PML growth-suppressor has an altered expression in human oncogenesis. *Oncogene* **10**, 1315-1324.
- Lallemand-Breitenbach, V., Zhu, J., Puvion, F., Koken, M., Honore, N., Doubeikovskiy, A., Duprez, E., Pandolfi, P. P., Puvion, E., Freemont, P. et al. (2001). Role of promyelocytic leukemia (PML) sumulation in nuclear body formation, 11S proteasome recruitment, and As2O3-induced PML or PML/retinoic acid receptor alpha degradation. *J. Exp. Med.* **193**, 1361-1371.



- Leung, A. K. and Lamond, A. I.** (2003). The dynamics of the nucleolus. *Crit. Rev. Eukaryot. Gene Expr.* **13**, 39-54.
- Lin, H. K., Bergmann, S. and Pandolfi, P. P.** (2004). Cytoplasmic PML function in TGF-beta signalling. *Nature* **431**, 205-211.
- Maul, G. G.** (1998). Nuclear domain **10**, the site of DNA virus transcription and replication. *BioEssays* **20**, 660-667.
- Prasanth, K. V., Sacco-Bubulya, P. A., Prasanth, S. G. and Spector, D. L.** (2003). Sequential entry of components of the gene expression machinery into daughter nuclei. *Mol. Biol. Cell* **14**, 1043-1057.
- Regad, T. and Chelbi-Alix, M. K.** (2001). Role and fate of PML nuclear bodies in response to interferon and viral infections. *Oncogene* **20**, 7274-7286.
- Roussel, P., Andre, C., Masson, C., Geraud, G. and Hernandez-Verdun, D.** (1993). Localization of the RNA polymerase I transcription factor hUBF during the cell cycle. *J. Cell Sci.* **104**, 327-337.
- Roussel, P., Andre, C., Comai, L. and Hernandez-Verdun, D.** (1996). The rDNA transcription machinery is assembled during mitosis in active NORs and absent in inactive NORs. *J. Cell Biol.* **133**, 235-246.
- Salomoni, P. and Pandolfi, P. P.** (2002). The role of PML in tumor suppression. *Cell* **108**, 165-170.
- Shiels, C., Islam, S. A., Vatcheva, R., Sasieni, P., Sternberg, M. J., Freemont, P. S. and Sheer, D.** (2001). PML bodies associate specifically with the MHC gene cluster in interphase nuclei. *J. Cell Sci.* **114**, 3705-3716.
- Sternsdorf, T., Jensen, K. and Will, H.** (1997). Evidence for covalent modification of the nuclear dot-associated proteins PML and Sp100 by PIC1/SUMO-1. *J. Cell Biol.* **139**, 1621-1634.
- Stuurman, N., de Graaf, A., Floore, A., Josso, A., Humbel, B., de Jong, L. and van Driel, R.** (1992). A monoclonal antibody recognizing nuclear matrix-associated nuclear bodies. *J. Cell Sci.* **101**, 773-784.
- Sugata, N., Li, S., Earnshaw, W. C., Yen, T. J., Yoda, K., Masumoto, H., Munekata, E., Warburton, P. E. and Todokoro, K.** (2000). Human CENP-H multimers colocalize with CENP-A and CENP-C at active centromere-kinetochore complexes. *Hum. Mol. Genet.* **9**, 2919-2926.
- Swedlow, J. R. and Hirano, T.** (2003). The making of the mitotic chromosome: modern insights into classical questions. *Mol. Cell* **11**, 557-569.
- Terris, B., Baldin, V., Dubois, S., Degott, C., Flejou, J. F., Henin, D. and Dejean, A.** (1995). PML nuclear bodies are general targets for inflammation and cell proliferation. *Cancer Res.* **55**, 1590-1597.
- Wang, J., Shiels, C., Sasieni, P., Wu, P. J., Islam, S. A., Freemont, P. S. and Sheer, D.** (2004). Promyelocytic leukemia nuclear bodies associate with transcriptionally active genomic regions. *J. Cell Biol.* **164**, 515-526.
- Wiesmeijer, K., Molenaar, C., Bekeir, I. M., Tanke, H. J. and Dirks, R. W.** (2002). Mobile foci of Sp100 do not contain PML: PML bodies are immobile but PML and Sp100 proteins are not. *J. Struct. Biol.* **140**, 180-188.
- Williams, J. M., Boyd, B., Nutikka, A., Lingwood, C. A., Barnett Foster, D. E., Milford, D. V. and Taylor, C. M.** (1999). A comparison of the effects of verocytotoxin-1 on primary human renal cell cultures. *Toxicol. Lett.* **105**, 47-57.
- Yeager, T. R., Neumann, A. A., Englezou, A., Huschtscha, L. I., Noble, J. R. and Reddel, R. R.** (1999). Telomerase-negative immortalized human cells contain a novel type of promyelocytic leukemia (PML) body. *Cancer Res.* **59**, 4175-4179.
- Zhong, S., Salomoni, P. and Pandolfi, P. P.** (2000). The transcriptional role of PML and the nuclear body. *Nat. Cell Biol.* **2**, E85-E90.